Received: 22 July 2019 | Revised: 5 May 2020 | Accepted: 5 May 2020

DOI: 10.1111/epi.16551

FULL LENGTH ORIGINAL RESEARCH

Epilepsia®

Modulation of posttraumatic epileptogenesis in aquaporin-4 knockout mice

Jenny I. Szu | **Dillon D. Patel** | **Som Chaturvedi** | **Jonathan W. Lovelace** | **Devin K. Binder**

Center for Glial-Neuronal Interactions, Division of Biomedical Sciences, School of Medicine, University of California, Riverside, Riverside, California, USA

Correspondence
Devin K. Binder, Division of Biomedical Sciences, School of Medicine, University of California, 1247 Webber Hall, Riverside, CA 92521.
Email: dbinder@ucr.edu

Abstract

Objective: To determine the role of aquaporin-4 (AQP4) in posttraumatic epileptogenesis using long-term video-electroencephalographic (vEEG) recordings. Here, differences in EEG were analyzed between wild-type (WT) and AQP4 knockout (KO) mice and between mice with and without posttraumatic epilepsy (PTE).

Methods: WT and AQP4 KO mice were subjected to a single controlled cortical impact traumatic brain injury (TBI) in the frontal cortex, and vEEG was recorded in the ipsilateral hippocampus at 14, 30, 60, and 90 days postinjury (dpi). Intrahippocampal electrical stimulation was also used to assess electrographic seizure threshold and electrographic seizure duration (ESD).

Results: The mean seizure frequency per day for WT mice was 0.07 ± 0.07, 0.11 ± 0.07, 0.26 ± 0.13, and 0.12 ± 0.10 at 14, 30, 60, and 90 dpi, respectively. The mean seizure frequency per day for AQP4 KO mice was 0.45 ± 0.27, 0.29 ± 0.12, and 0.26 ± 0.19 at 14, 30, and 60 dpi, respectively. The mean seizure duration was 15 ± 2 seconds and 24 ± 3 seconds for WT and AQP4 KO mice, respectively. The percentage of mice that developed PTE were 28% and 37% for WT and AQP4 KO mice, respectively. Power spectral density (PSD) analysis revealed alterations in EEG frequency bands between sham and TBI in both genotypes. Additionally, PSD analysis of spontaneous recurrent seizures revealed alterations in delta power between genotypes. Morlet wavelet analysis detected heterogeneity in EEG seizure subtypes and dynamic EEG power patterns after TBI. Compared with AQP4 KO mice, a significant increase in ESD was observed in WT mice at 14 dpi.

Significance: Posttraumatic seizures (PTSs) may be modulated by the astrocyte water channel AQP4. Absence of AQP4 increases the number of spontaneous seizures, increases seizure duration, and alters EEG power patterns of PTSs.

KEYWORDS

aquaporin-4, electrographic seizure duration, electrographic seizure threshold, posttraumatic epilepsy, power spectral density, spontaneous recurring seizures

1 | INTRODUCTION

Posttraumatic epilepsy (PTE) is a neurological disorder where late spontaneous recurrent seizures (SRSs) develop following a traumatic brain injury (TBI).[1] PTE makes up ~20% of symptomatic epilepsy[2,3] and 6% of all epilepsies.[4] Clinical studies showed that PTE can manifest as temporal lobe epilepsy (TLE),[5] and spontaneous and hilar-evoked epileptiform activity[6,7] and granule cell hyperexcitability[5,8] have been observed in experimental models of TBI. These studies support the significance of the hippocampus and its increased susceptibility to neuronal hyperexcitability after injury.

In vivo electrophysiological changes in the hippocampus after experimental TBI using the controlled cortical impact (CCI) injury model have not been well characterized. Studies of PTE using CCI in adult and pediatric mice have induced the injury in a similar location (parietotemporal region directly above the hippocampus) and monitored SRSs using cortical screw electrodes.[6,7,9–12] Whereas these studies validate increased seizure susceptibility in the cortex after TBI, none has examined the development of SRSs in the highly sensitive hippocampus. Furthermore, TBI induction at a similar location diminishes the translational aspect of these studies, as the frontal cortex has been shown to be highly vulnerable to brain injuries.[13–16] The probability of late posttraumatic seizures (PTSs) from a unilateral contusion in the frontal, temporal, and parietal locations is 20%, 16%, and 19%, respectively.[17]

Found highly polarized to astrocytic endfeet in contact with blood vessels, the small integral membrane protein aquaporin-4 (AQP4) facilitates the bidirectional transport of water in response to an osmotic gradient.[18–21] Mice lacking AQP4 have normal development, growth, and survival as well as similar brain morphology and blood-brain barrier integrity as wild-type (WT) mice.[22,23] However, a minor deficit in urinary concentration,[22] impaired hearing, mild retinal dysfunction,[24] and decreased osmotic water permeability[25] were observed in the absence of AQP4. Additionally, mice lacking AQP4 exhibited increased extracellular space,[26] altered K^+ homeostasis,[27] increased electrical stimulation–induced seizure threshold and duration,[27] and increased seizure frequency after induction of status epilepticus,[28] functions critical in epilepsy.

In the present study, we first aimed to determine whether a single episode of TBI in the frontal cortex could lead to SRSs in the hippocampus and PTE. Second, using AQP4 knockout (KO) mice, we sought to determine whether AQP4, which is known to regulate seizure susceptibility in other models,[27,29] also regulates PTE.

Key Points

- AQP4 KO mice have significantly longer spontaneous recurrent seizure duration
- ESD is significantly higher in WT mice at 14 dpi
- Morlet wavelet analysis revealed heterogeneity in EEG power after TBI
- The astrocyte channel AQP4 may potentially modulate PTSs after TBI

2 | MATERIALS AND METHODS

2.1 | Animals

All experiments were conducted in accordance with the guidelines set forth by the National Institutes of Health and approved by the University of California, Riverside Institutional Animal Care and Use Committee. Eight- to 10-week-old male CD1 WT and AQP4 KO mice of the same background were used for all experiments. AQP4 KO mice were generated as previously described.[22] Mice were housed under controlled conditions (12-hour light/dark cycle) with ad libitum access to water and food.

Fifty-three WT mice and 72 AQP4 KO mice received a TBI, with AQP4 KO mice having a significantly greater mortality (25%) compared to WT mice (11%; $P = .0159$, Fisher exact test). A total of 95 WT mice (n = 47 TBI and n = 48 sham) and 96 AQP4 KO mice (n = 54 TBI and n = 42 sham) were used. Due to limited video-electroencephalographic (vEEG) recording devices, a subset of mice from each genotype, treatment, and timepoint underwent vEEG recordings. The number of mice that underwent vEEG are n = 12, 6, 14, and 7 for WT sham, n = 8, 10, 11, and 7 for WT TBI, n = 9, 12, 4, and 7 for AQP4 KO sham, and n = 7, 13, 6, and 4 for AQP4 KO TBI at 14, 30, 60, and 90 days postinjury (dpi), respectively.

2.2 | Surgical preparation

Mice were anesthetized with an intraperitoneal injection of ketamine (80 mg/kg) and xylazine (10 mg/kg). Additional anesthesia was administered when necessary. Mice were then immobilized onto a stereotactic frame, and a midline incision was made and reflected.

2.3 | CCI injury

A high-speed surgical hand drill with a ¼-mm straight handpiece-sized carbide bur (S.S. White Technologies)

was used to create a 2 × 2-mm^2 craniotomy (~0.5 mm rostral and lateral from bregma) over the right frontal cortex with the dura intact. With a 2-mm impactor tip, the CCI device (Leica Biosystems) induced a moderate-severe TBI onto the exposed brain at a velocity of 5 m/s, with a depth of 1 mm and a contact time of 200 milliseconds. After TBI, the skull flap was carefully replaced and the incision was sutured. Mice were then allowed to recover over a temperature-controlled heating pad. Sham controls received a craniectomy only.

2.4 | Electrode preparation

A three-channel two twisted bipolar stainless-steel electrode with a diameter of 0.010 in (P Technologies) was used for all EEG implantations and prepared as previously described.[30] The 2-mm twisted bipolar wires were implanted in the ipsilateral dorsal hippocampus, and the 0.5-mm untwisted wire was used to ground in the cortex. To achieve reliable EEG recordings, ~0.5 mm of the insulating coat at the distal tip of the wires was removed.

2.5 | Electrode implantation

Mice underwent EEG implantation surgery 10 days prior to their final timepoint (14, 30, 60, and 90 dpi). Mice were immobilized in a stereotactic frame, and the skull was cleaned with normal saline. Etching gel (Clearfil Photobond, Kuraray) was applied to the skull and washed with normal saline. Stereotaxic coordinates of the hippocampus were identified,[31] and a craniectomy of ~2 mm in diameter was created. The dura was gently removed, and bonding agent (Clearfil Photobond, Kuraray) was applied onto the skull and light cured. The pedestal of the electrode was lowered into the ipsilateral dorsal hippocampus (anteroposterior = −1.8 mm, mediolateral = +1.6 mm from bregma) until the implant pedestal rested on top of the skull. Dental cement (PANAVIA SA Cement, Kuraray) was used to secure the electrode in place. Mice were allowed to recover for 3 days following surgery completion.

2.6 | Continuous vEEG data acquisition

vEEG acquisition began after the recovery period and lasted 7 days. Mice were single housed with access to food and water ad libitum and freely moving during vEEG acquisition. Behavioral activity was video monitored with a megapixel internet protocol camera (high definition 1080P) with infrared light-emitting diode for nighttime recording (ELP1 closed circuit television) and time-synced with EEG recording. Mice were recorded using either our customized wireless EEG sensor (Epoch) or a tethered system (BioPac). For wireless EEG recording, the electrode pedestal was connected to a wireless transmitter (Epoch) with the cage on top of a receiver tray. The number of mice recorded with the wireless system were n = 1, 3, 12, and 4 for WT sham, n = 0, 7, 9, and 5 for WT TBI, n = 1, 8, 4, and 3 for AQP4 KO sham, and n = 7, 5, 1, and 2 for AQP4 KO TBI at 14, 30, 60, and 90 dpi, respectively. For tethered EEG recording, mice were connected to the acquisition system via a commutator to allow for freedom of motion. The number of mice recorded with the tethered system were n = 11, 3, 2, and 3 for WT sham, n = 8, 3, 2, and 2 for WT TBI, n = 8, 4, 0, and 4 for AQP4 KO sham, and n = 0, 8, 5, and 2 for AQP4 KO TBI at 14, 30, 60, and 90 dpi, respectively. Both wireless and tethered EEG recordings were acquired using a digital acquisition system (MP150 or MP160, AcqKnowledge 4.4 or 5 software; BioPac). Normal EEG output was amplified with a gain of 5000, bandpass filtered from 0.1 to 35 Hz, and digitized at 625 samples/s.

Electrographic SRSs from the 1-week vEEG recordings were manually identified and confirmed by two blinded observers. Spontaneous seizures were defined as spiking epileptiform activity lasting continuously for at least 5 seconds at a frequency of ≥3 Hz.[28] Electrographic seizures were correlated with corresponding time-synced video for behavioral assessment based on the modified Racine scale. Mice with one or more (ie, recurrent) late spontaneous seizures, PTSs occurring 1 week after the initial TBI, were classified as having PTE (so as to accomplish stringent PTE identification consistent with the literature).

2.7 | Intrahippocampal electrical stimulation

Upon completion of vEEG, mice underwent in vivo intrahippocampal electrical stimulation for the quantitative assessment of electrographic seizure threshold (EST) and electrographic seizure duration (ESD) at each experimental endpoint. Mice were connected to a tethered EEG system as described above, and electrical stimulations were delivered with a stimulus isolator (World Precision Instruments Linear Stimulus Isolator A395). Electrical stimulation was applied as previously described[27] after a 15-minute EEG baseline. Each electrical stimulation consisted of a 60-Hz, 1-second train of 1-millisecond biphasic square-wave pulses.[27] Stimulation intensity increased incrementally by 20 μA every 2 minutes starting at 20 μA. EST was recorded as the threshold at which a hippocampal seizure of at least 5 seconds was observed. ESD was recorded as the total duration of the electrographic seizure at the determined EST.

2.8 | Seizure frequency, duration, and incidence of PTE

The mean seizure frequency was determined for all mice that received a TBI. For each animal, the seizure frequency was determined as the total number of seizures/total number of vEEG recording days. The seizure frequency at each timepoint for each genotype was analyzed with one-way analysis of variance (ANOVA) with Bonferroni post hoc analysis, and the seizure frequency at each timepoint between genotypes was analyzed with two-way ANOVA with Bonferroni post hoc analysis. The mean seizure duration was determined for each genotype and differences were analyzed using the Mann-Whitney *U* test. All mice that displayed SRSs were considered to have PTE, and the total percentage of mice with PTE was determined for each genotype. Comparisons in the percentage of mice that developed PTE between genotypes were analyzed with Fisher exact test. All error bars are represented as mean ± SEM, and differences were considered statistically significant at $P < .05$.

2.9 | Power spectral density analysis

All power spectral density (PSD) analysis was performed blinded. Resting EEG data acquired during the 1-week period was extracted from AcqKnowledge software (Biopac), and PSD was analyzed using BrainVision Analyzer 2.1 (Brain Products). Due to the large dataset acquired during the 1-week vEEG recording, 20-hour bins were selected at random from each EEG recording for analysis. The number of 20-hour bins analyzed for each timepoint were n = 47, 32, 30, and 8 for WT sham, n = 38, 42, 78, and 19 for WT TBI, n = 30, 35, 17, and 28 for AQP4 KO sham, and n = 30, 49, 31, and 16 for AQP4 KO TBI at 14, 30, 60, and 90 dpi, respectively. Artifacts were removed with semiautomatic procedure based on maximum-minimum, low activity, and amplitude criteria. EEG signals were then divided into 10-second segments, and fast Fourier transform (FFT) was applied on each segment at 1-Hz resolution from 1 to 35 Hz to generate frequency values. EEG frequency bands were as follows: delta (1-3 Hz), theta (4-7 Hz), alpha (8-14 Hz), and beta (15-35 Hz). FFT results were then extracted from BrainVision Analyzer 2.1 and averaged using customized MATLAB scripts (MathWorks).

PSD analysis was also investigated for all PTSs with FFT performed for each PTS at 1-Hz resolution from 1 to 35 Hz to generate frequency values. EEG frequency bands were determined as described previously. The number of PTSs analyzed for each timepoint was n = 4, 8, 20, and 6 for 14, 30, 60, and 90 dpi, respectively for WT mice and n = 19, 24, and 11, for 14, 30, and 60 dpi, respectively for AQP4 KO mice.

Differences in each EEG frequency band from resting EEG were compared between sham and TBI at all timepoints for each genotype and for PTSs between genotypes using two-way ANOVA with Bonferroni post hoc analysis. All error bars are represented as mean ± SEM, and differences were considered statistically significant at $P < .05$.

2.10 | Morlet wavelet analysis

Quantitative analysis for confirmed PTSs was processed for Morlet wavelets from 1 to 35 Hz using power density (μV/Hz) 10 seconds before and after seizure onset (BrainVision Analyzer 2.1) and Morelet wavelets were then qualitatively analyzed. A Morlet parameter of 15 was used to provide the most ideal frequency/power discrimination. Grand averages of Morlet wavelets were performed for all PTSs at each timepoint for both genotypes (n = 4, 8, and 20 for 14, 30, and 60 dpi, respectively for WT mice and n = 19, 24, and 11, for 14, 30, and 60 dpi, respectively for AQP4 KO mice). Because AQP4 KO mice did not exhibit any PTSs at 90 dpi, Morlet wavelets from WT mice at 90 dpi were excluded from direct comparison with AQP4 KO mice.

2.11 | EST and ESD

To estimate the effect of injury alone, EST and ESD of TBI groups at each timepoint were normalized to the average EST and ESD of its sham counterparts. Comparisons of normalized EST and ESD between genotypes were performed with two-way ANOVA with Bonferroni post hoc analysis. All error bars are represented as mean ± SEM, and differences were considered statistically significant at $P < .05$. Due to technical challenges for this experimental paradigm, not all mice were recorded successfully. Mice with poor electrical stimulation EEG recordings were excluded from analysis. The resulting n's for all timepoints are n = 7, 5, 5, and 7 for WT sham, n = 9, 6, 12, and 11 for WT TBI, n = 5, 6, 5, and 12 for AQP4 KO sham, and n = 7, 7, 7, and 11 for AQP4 KO TBI at 14, 30, 60, and 90 dpi, respectively.

All statistical analysis was performed using GraphPad Prism 8.

3 | RESULTS

3.1 | Electrographic and behavioral characteristics of SRSs

Late PTSs must be observed at least 1 week after the initial trauma to establish a working model of PTE. Electrographic SRSs were detected at each timepoint after TBI and correlated with corresponding video for behavioral assessment. Similar injury severity was observed qualitatively between

both WT and AQP4 KO mice, as reported in our recent studies based on increased glial fibrillary acidic protein immunoreactivity,[32] which may contribute to the similar behavioral seizures observed. Nonconvulsive seizures paralleled the electrographic seizures, and behavioral seizures were primarily motor arrest with occasional facial clonus. In rare cases, mice exhibited tail stiffness, limb clonus, and incessant grooming. Sham mice remained seizure-free with the exception of one mouse in each genotype that displayed a single seizure at 60 days (WT) and 14 days (AQP4 KO) postcraniectomy. No sham mice exhibited PTE.

Electrographically, most seizures were of the "fast polyspike" subtype, where seizure onset was sudden, with increased frequency and amplitude, and seizure termination was followed by a postictal depression or return to baseline (Figure 1A). The "ramp-up" seizure subtype initiated from baseline (Figure 1B[1-2]), gradually developed into a full seizure, and was followed by a postictal depression at the termination of the seizure (Figure 1B[3]). The "low-frequency" seizure subtype displayed high-amplitude spikes that appeared abruptly and were followed by return to baseline at the conclusion of the seizure (Figure 1C). In total, WT mice exhibited 32 fast polyspikes, 0 ramp-up seizures, and six low-frequency seizures, whereas AQP4 KO mice displayed 51 fast polyspikes, two ramp-up seizures, and one low-frequency seizure.

3.2 | AQP4 KO mice have increased spontaneous seizure duration

Table 1 summarizes the seizure frequency, duration, and percent of PTE. The mean seizure frequency per day for WT mice was 0.07 ± 0.07, 0.11 ± 0.07, 0.26 ± 0.13, and 0.12 ± 0.10 at 14, 30, 60, and 90 dpi, respectively and for AQP4 KO mice was 0.45 ± 0.27, 0.29 ± 0.12, and 0.26 ± 0.19 at 14, 30, and 60 dpi, respectively. Seizure frequency between timepoints was not statistically different for each genotype ($P = .5722$ WT; $P = .5491$, AQP4 KO; one-way ANOVA) and between genotypes (no main effects on time and genotype or interaction). AQP4 KO mice had significantly longer seizure duration (24 ± 3 seconds) compared with WT (15 ± 2 seconds, $P = .0133$). The percentage of mice that developed PTE were

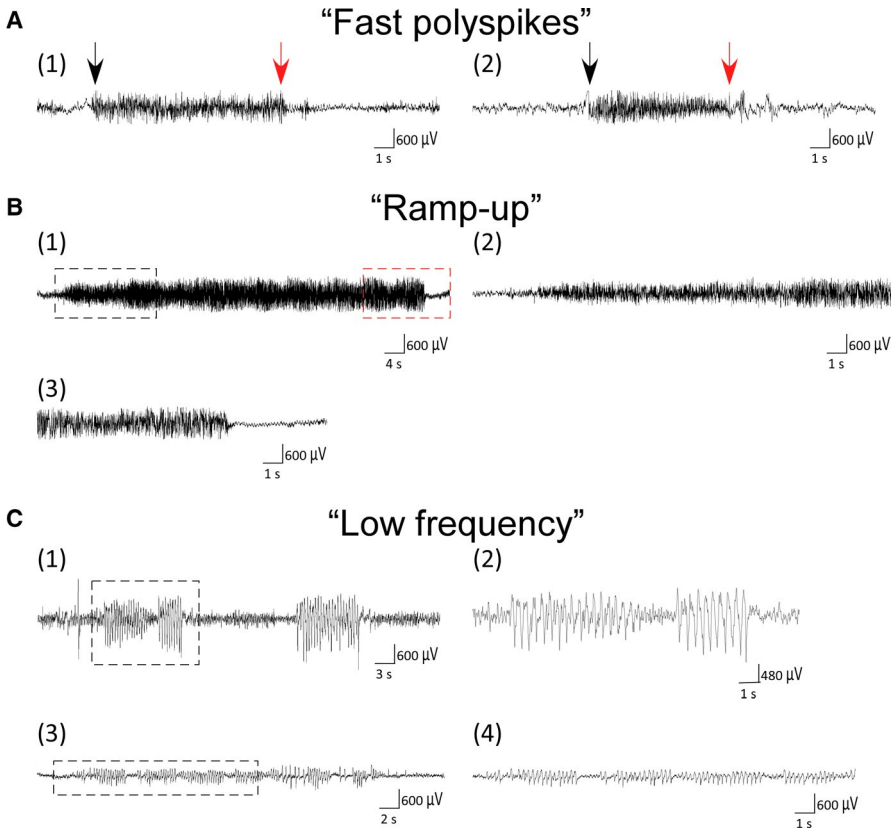

FIGURE 1 Subtypes of electrographic spontaneous posttraumatic seizures. A, Examples of "fast polyspike" seizures in wild-type (WT) mice at 60 days postinjury (dpi; 1, 2). These electrographic seizures appear suddenly and have markedly increased frequency and amplitude compared with baseline. Termination of the seizure is often followed by a postictal depression or return to baseline. Black arrows = seizure onset; red arrows = seizure termination. B, Example of a seizure that developed gradually from baseline from an aquaporin-4 (AQP4) knockout (KO) mouse at 30 dpi. The expanded view of the beginning of the seizure (dashed black box) is shown in (2), and the end of the seizure (dashed red box) is shown in (3); this was followed by a postictal depression and return to baseline. C, Examples of "low-frequency" seizures in a WT mouse at 14 dpi (1) and an AQP4 KO mouse at 60 dpi (3). Expanded views of individual high-amplitude spikes denoted by dashed black boxes in (1) and (3) are shown in (2) and (4), respectively

TABLE 1 Summary of seizure frequency, duration, and PTE

	14 dpi	30 dpi	60 dpi	90 dpi
Mean seizure frequency, seizures/d				
WT	0.07 ± 0.07	0.11 ± 0.07	0.26 ± 0.13	0.12 ± 0.10
AQP4 KO	0.45 ± 0.27	0.29 ± 0.12	0.26 ± 0.19	
Mean seizure duration, s				
WT	15 ± 2			
AQP4 KO	24 ± 3			
Total with PTE				
WT	28%			
AQP4 KO	37%			

Note: Seizure frequency was not statistically different between timepoints for each genotype and between genotypes. AQP4 KO mice exhibited a significantly longer seizure duration compared to WT mice ($P = .0133$). The percentage of mice that developed PTE was not statistically different between genotypes. Data are represented as mean ± SEM.

Abbreviations: AQP4, aquaporin-4; dpi, days postinjury; KO, knockout; PTE, posttraumatic epilepsy; WT, wild-type.

28% (10/36 WT mice) and 37% (11/30 AQP4 KO mice) and were not statistically different ($P = .2270$, Fisher exact test).

3.3 | TBI increases resting EEG power

In WT mice, a main effect of interaction ($F_{3, 286} = 3.693$, $P = .0123$) was observed in the delta frequency band, with a significant difference between sham and TBI groups at 14 dpi ($P = .0169$). A main effect of treatment was detected in the theta frequency band ($F_{1, 286} = 5.110$, $P = .0245$) and alpha frequency band ($F_{1, 286} = 7.732$, $P = .0058$); however, there were no significant differences between sham and TBI groups at all timepoints. In the beta frequency band, a main effect of treatment was revealed ($F_{1, 286} = 8.843$, $P = .0032$) and a significant difference between sham and TBI groups at 30 dpi was detected ($P = .0341$; Figure 2A).

In AQP4 KO mice, a main effect of interaction ($F_{3, 207} = 5.208$, $P = .0017$) and time ($F_{3, 207} = 13.90$, $P < .0001$) was detected in the delta frequency band and a significant difference between sham and TBI groups at 14 dpi ($P = .0014$). In the theta frequency band, a main effect of interaction ($F_{3, 228} = 4.714$, $P = .0033$), time ($F_{3, 228} = 4.893$, $P = .0026$), and treatment ($F_{1, 228} = 16.24$, $P < .0001$) was detected and significant differences were observed between sham and TBI groups at 14 ($P = .0021$) and 90 dpi ($P = .0005$). Similarly, a main effect of interaction ($F_{3, 228} = 3.985$, $P = .086$), time ($F_{3, 228} = 7.067$, $P = .0001$), and treatment ($F_{1, 228} = 5.743$, $P = .0174$) was revealed at the alpha frequency band and a significant difference was observed between sham and TBI groups at 90 dpi ($P = .195$). In the beta frequency band, a main effect of time was observed ($F_{3, 228} = 9.958$, $P < .0001$); however, no significant differences between sham and TBI groups at all timepoints was observed (Figure 2B).

3.4 | PTSs exhibit EEG power differences in the delta frequency band

PTS PSD analysis revealed main effects of frequency ($F_{3, 360} = 11.13$, $P < .0001$) and genotype ($F_{1, 360} = 7.174$, $P = .0077$), and a significant difference in the delta frequency band between genotypes was observed ($P = .0017$; Figure 2C).

3.5 | Morlet wavelet analysis reveals distinct patterns in EEG power

Morlet wavelet analysis revealed EEG power heterogeneity for different seizure morphologies. The fast polyspike seizure subtype exhibited Morlet wavelets with a sudden increase in power across both time and frequency at seizure initiation (Figure 3A). The ramp-up seizure subtype also presented an increase in EEG power at seizure onset that was more apparent in the Morlet wavelets than in the raw EEG (Figure 3B). Finally, the low-frequency seizure subtype exhibited Morlet wavelets with EEG power at the lower frequencies (~5-15 Hz), where each EEG spike closely mirrored a Morlet wavelet pattern (Figure 3C).

Morlet wavelet analysis also detected different EEG power patterns at each timepoint in both genotypes. In WT mice, EEG power was predominantly at the lower frequencies (~5-15 Hz) at 14 dpi, which was contributed by the low-frequency seizure subtype. Additionally, the low EEG power observed prior to seizure onset was caused by individual spikes occurring before the start of the seizures. Low EEG power was consistent across time and frequency at 30 and 60 dpi. In contrast, AQP4 KO mice displayed consistent low EEG power all timepoints (Figure 4).

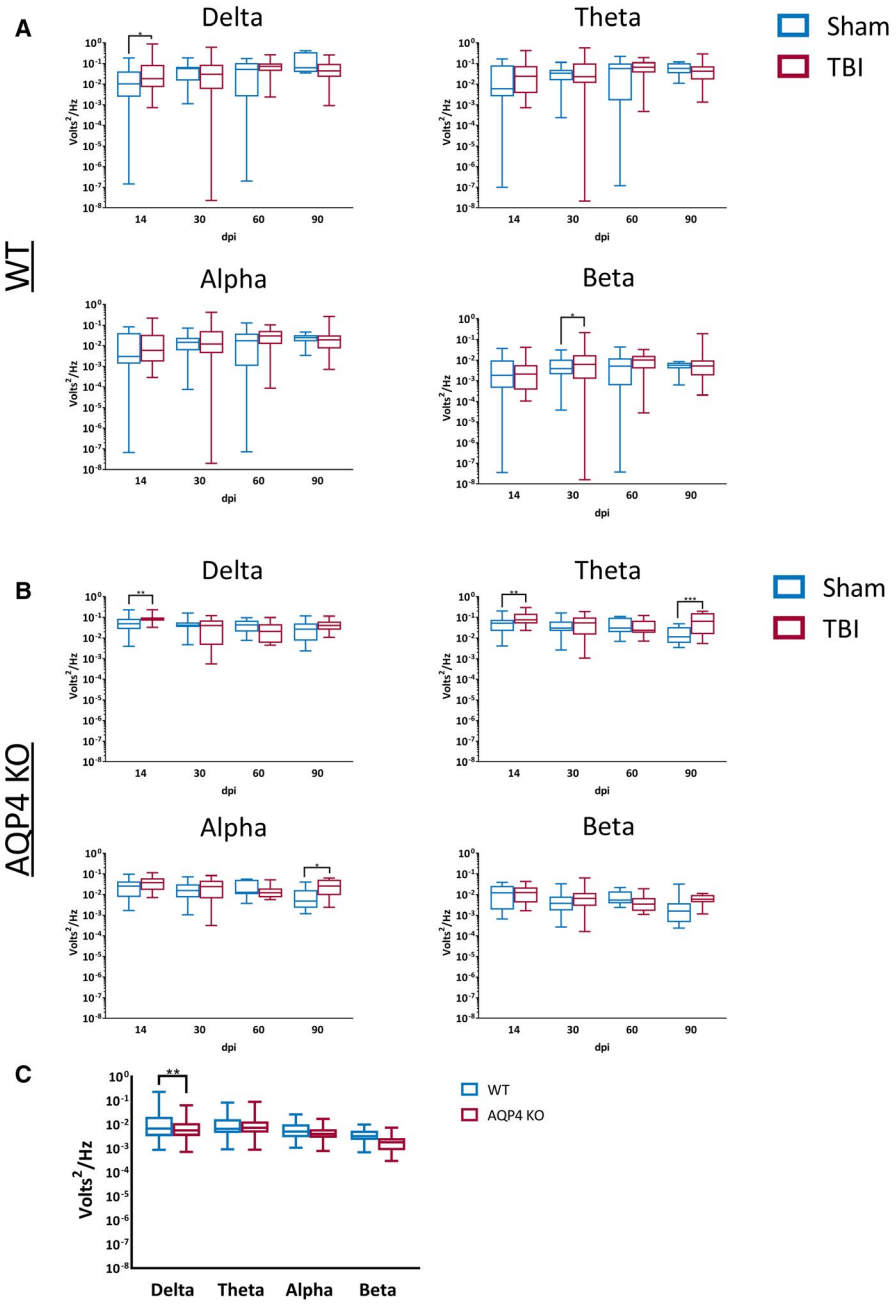

FIGURE 2 Altered electroencephalographic (EEG) power spectra after traumatic brain injury (TBI). A, Wild-type (WT) mice exhibited a significant increase in the delta frequency band at 14 days postinjury (dpi) and in the beta frequency band at 30 dpi. B, Aquaporin-4 (AQP4) knockout (KO) mice exhibited an increase in the delta frequency band at 14 dpi, in the theta frequency band at 14 and 90 dpi, and in the alpha frequency band at 90 dpi. C, EEG power spectra of posttraumatic seizures revealed a significant increase in the delta frequency band at 14 dpi of WT mice compared with AQP4 KO mice. $^{*}P < .05$, $^{**}P < .01$, $^{***}P < .001$. Error bars indicate mean ± SEM. Delta = 1-3 Hz, theta = 4-7 Hz, alpha = 8-14 Hz, and beta = 15-35 Hz

3.6 | EST and ESD

No significant differences in normalized EST were observed between WT and AQP4 KO mice. A main effect of time ($F_{3, 62} = 3.439$, $P = .0221$) and interaction ($F_{3, 62} = 4.2569$, $P = .0084$) was observed in normalized ESD, with a significant increase at 14 dpi in WT mice ($P = .0033$; Figure 5).

4 | DISCUSSION

We sought to determine whether a single episode of TBI in the frontal cortex could lead to the development of PTE. First, we found that a single TBI in the frontal cortex can lead to SRSs in the ipsilateral hippocampus, which correlated with nonconvulsive seizures. Second, we found that AQP4 KO mice exhibited significantly longer seizure duration compared with WT mice. Third, we observed altered EEG power spectra in both genotypes as well as an increase in the delta frequency band of PTSs between genotypes. Fourth, Morlet wavelet analysis detected heterogeneity in EEG seizure subtypes. Fifth, we found significant differences in ESD between WT and AQP4 KO mice at 14 dpi. We recognize our sampling size is limited; nevertheless, we report significant findings that may yield insight into potential mechanisms of AQP4 modulation in PTE.

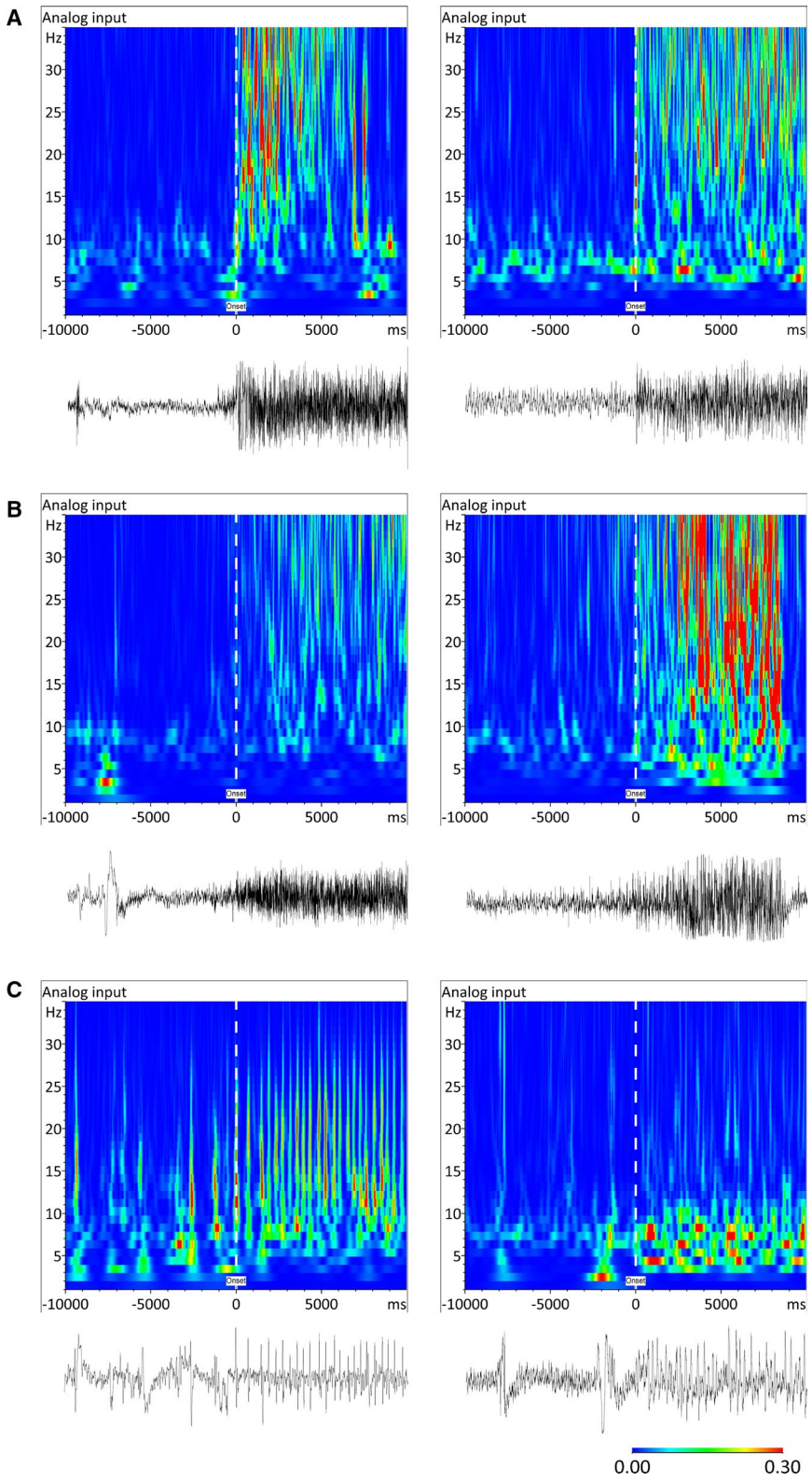

FIGURE 3 Distinct seizure morphologies revealed by Morlet wavelet analysis. A, Morlet wavelets for "fast polyspike" seizures. An increase in electroencephalographic (EEG) power is detected at seizure onset. B, Morlet wavelets for "ramp-up" seizures that developed gradually from baseline. An increase in EEG power was observed during seizure onset. Moreover, Morlet wavelet analysis was able to distinguish a clear seizure onset compared to viewing the raw EEG alone. C, Morlet wavelets for "low-frequency" seizures. As expected, this seizure subtype has EEG power at the lower frequencies (~5-15 Hz) and Morlet wavelet pattern is closely associated with each EEG spike. The vertical axis represents frequency from 1 to 35 Hz, and the horizontal axis represents time in milliseconds. Dashed vertical white line indicates seizure onset

4.1 | PTS modulation by AQP4

Seizure activity and epilepsy have profound effects on synaptic plasticity[33,34]; however, whether synaptic plasticity is altered in PTE remains unclear. Moreover, the role of AQP4 in synaptic plasticity and its contributions to PTE are of great interest. Previous reports found that AQP4 KO mice exhibited reduced brain-derived neurotrophic factor (BDNF)-dependent long-term potentiation (LTP) and that BDNF scavengers or Trk receptor inhibitors can rescue long-term depression.[35] This suggests that neurotrophins are dysregulated in the absence of AQP4, leading to

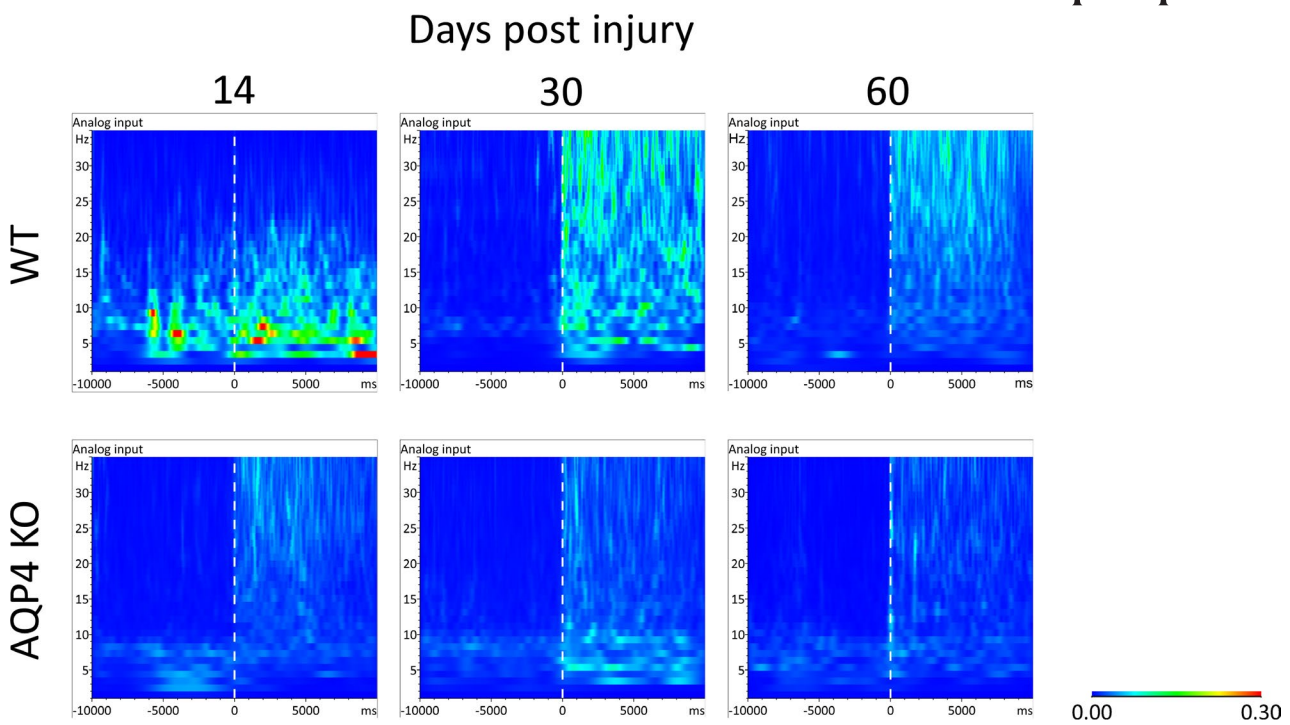

FIGURE 4 Grand averages of Morlet wavelets after traumatic brain injury (TBI). Morlet wavelet analysis revealed distinct electroencephalographic (EEG) patterns between wild-type (WT) and aquaporin-4 (AQP4) knockout (KO) mice after TBI. In WT mice, EEG power was mainly localized to the lower frequencies (~5-15 Hz) at 14 days postinjury (dpi). The low EEG power observed prior to seizure onset was contributed by individual spikes occurring before the start of the seizure. At 30 and 60 dpi, low EEG power was consistent across both time and frequency. In AQP4 KO mice, overall EEG power was low and was seemingly consistent across both time and frequency at 14, 30, and 60 dpi. As AQP4 KO mice did not exhibit any spontaneous seizures at 90 dpi, Morlet wavelet analysis was only directly compared at 14, 30, and 60 dpi between genotypes. On the scale bar, warm colors indicate higher power and cool colors indicate lower power

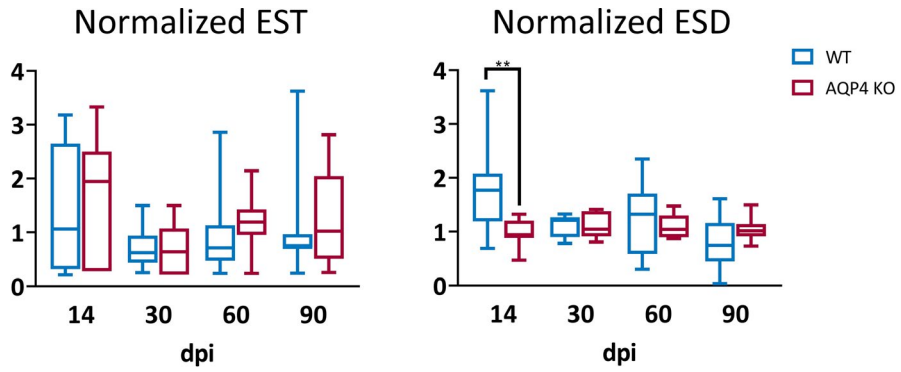

FIGURE 5 Increased stimulation-induced electrographic seizure duration in wild-type (WT) mice. No significant differences in normalized electrographic seizure threshold (EST; left) was observed between WT and aquaporin-4 (AQP4) knockout (KO) mice at each timepoint. A significant increase in normalized electrographic seizure duration (ESD; right) was detected in WT mice compared with AQP4 KO mice at 14 days postinjury (**$P = .0033$). EST and ESD TBI groups are normalized to shams. Error bars indicate mean ± SEM

abnormal synaptic plasticity. Therefore, the lack of AQP4 may inhibit secretion of BDNF, which impairs LTP and increases seizure activity.

Mislocalization of AQP4 may also contribute to the development of PTE. Loss of perivascular AQP4 was detected in postmortem sclerotic hippocampi of patients with mesial TLE,[36] although an overall increase in AQP4 expression was observed.[37] Loss of perivascular AQP4 has also been documented in rodent models of TLE[38–40] and TBI.[41] The dysregulation of AQP4 can impair water and ion homeostasis, thereby swelling astrocyte endfeet and increasing seizure susceptibility.[42] Recently, we found the greatest loss of perivascular AQP4 at 14 dpi, with partial restoration at 30 dpi and full recovery by 60 dpi.[32] This suggests that AQP4

mislocalization at earlier timepoints may contribute to PTE at chronic timepoints. Although not statistically significant, AQP4 KO mice displayed increased seizure frequency compared with WT mice. AQP4 KO mice also did not develop SRSs at 90 dpi. This indicates that the absence and/or redistribution of AQP4 can perturb water and ion equilibrium, increasing neuronal hyperexcitability and seizure duration, which may be compensated through other mechanisms (eg, feed-forward inhibition networks) to attenuate seizure activity at a later time.

4.2 | Modulation of EEG power in PTSs by AQP4

We found that TBI caused an increase in hippocampal EEG delta and theta power at earlier timepoints (14 and 30 dpi), which may be correlated with information processing. Patients undergoing seizure monitoring reported increased hippocampal delta/theta oscillations that were associated with spatial processing.[43] Therefore, hippocampal spatial memory may be altered in PTE, which can be further exacerbated in the absence of AQP4. Interestingly, memory and cognitive deficits have been reported in AQP4 KO mice.[44]

With the limited EEG data that were analyzed, particularly at 90 dpi, a thorough interpretation of EEG power spectra cannot be ascertained. Nevertheless, our current findings at the earlier timepoints suggest changes in hippocampal connectivity that may influence other frequency rhythms at chronic timepoints. Future studies with greater n's and utilizing behavioral assays can elucidate the correlation between PTE and cognitive functions as well as examine alterations in higher-frequency rhythms (eg, low and high gamma).

4.3 | PTSs have varying Morlet wavelet patterns

To explore the nonstationary complexity of ictal events, we applied Morlet wavelet analysis on each PTS. Morlet wavelet analysis revealed two key findings: (1) patterns in EEG power are heterogeneous in seizures with different subtypes and (2) EEG power is lower in AQP4 KO mice. Surprisingly, although AQP4 KO mice exhibited lower EEG power, they still displayed more PTSs and greater incidence of PTE compared with WT mice. These findings demonstrate the potential application of Morlet wavelet analysis to move beyond using traditional EEG to identify EEG abnormalities to more clearly distinguish between different electrographic seizure subtypes and patterns during pathological states such as PTE.

4.4 | TBI increases seizure duration at acute timepoints

Studies have demonstrated increased seizure susceptibility and severity of behavioral seizures after TBI using pentylenetetrazole (PTZ).[8,9] In our studies, we tested seizure susceptibility using the well-established intrahippocampal electrical stimulation model[27] rather than pharmacologically with PTZ. This method allows an unbiased and quantitative analysis of seizure susceptibility, and we are the first to employ this technique in an animal model of PTE. Interestingly, we did not detect any differences in normalized EST between groups and at each timepoint. This may be because we did not observe overt morphological changes in the hippocampus (data not shown) to significantly decrease seizure threshold. Surprisingly, we only detected significant differences in normalized ESD between genotypes at 14 dpi, although studies using similar protocols revealed a significant increase in ESD in naive AQP4 KO mice compared with naive WT mice.[27] One plausible explanation may be that AQP4 KO mice are protected from secondary injuries such as cerebral edema.[45] Therefore, at earlier timepoints, AQP4 KO mice may not have developed significant edema after TBI, thereby reducing duration of electrical stimulation–induced seizures.

5 | CONCLUSIONS

We found that a single TBI in the frontal cortex can lead to hippocampal SRSs and mice lacking AQP4 exhibited significantly longer seizure duration compared with WT mice. Future studies utilizing this TBI model can examine mechanistic effects of AQP4 modulation to determine whether AQP4 may be a promising therapeutic target for PTE.

CONFLICT OF INTEREST

None of the authors has any conflict of interest to disclose. We confirm that we have read the Journal's position on issues involved in ethical publication and affirm that this report is consistent with those guidelines.

AUTHOR CONTRIBUTIONS

J.I.S. and D.K.B. both participated in the experimental design. J.I.S. performed all the experiments, and all authors participated in data analysis. J.I.S. drafted and D.K.B. edited the manuscript.

ORCID

Devin K. Binder https://orcid.org/0000-0003-1597-5604

REFERENCES

1. Pitkänen A, McIntosh TK. Animal models of post-traumatic epilepsy. J Neurotrauma. 2006;23:241–61.

2. Engel J Jr. A proposed diagnostic scheme for people with epileptic seizures and with epilepsy: report of the ILAE Task Force on Classification and Terminology. Epilepsia. 2001;42:796–803.
3. Lowenstein DH. Epilepsy after head injury: an overview. Epilepsia. 2009;50(Suppl 2):4–9.
4. Hauser WA, Annegers JF, Kurland LT. Incidence of epilepsy and unprovoked seizures in Rochester, Minnesota: 1935–1984. Epilepsia. 1993;34:453–68.
5. Santhakumar V, Ratzliff AD, Jeng J, Toth Z, Soltesz I. Long-term hyperexcitability in the hippocampus after experimental head trauma. Ann Neurol. 2001;50:708–17.
6. Hunt RF, Scheff SW, Smith BN. Posttraumatic epilepsy after controlled cortical impact injury in mice. Exp Neurol. 2009;215:243–52.
7. Hunt RF, Scheff SW, Smith BN. Regionally localized recurrent excitation in the dentate gyrus of a cortical contusion model of posttraumatic epilepsy. J Neurophysiol. 2010;103:1490–500.
8. Golarai G, Greenwood AC, Feeney DM, Connor JA. Physiological and structural evidence for hippocampal involvement in persistent seizure susceptibility after traumatic brain injury. J Neurosci. 2001;21:8523–37.
9. Bolkvadze T, Pitkänen A. Development of post-traumatic epilepsy after controlled cortical impact and lateral fluid-percussion-induced brain injury in the mouse. J Neurotrauma. 2012;29:789–812.
10. Pijet B, Stefaniuk M, Kostrzewska-Ksiezyk A, Tsilibary P-E, Tzinia A, Kaczmarek L. Elevation of MMP-9 levels promotes epileptogenesis after traumatic brain injury. Mol Neurobiol. 2018;55:9294–306.
11. Guo D, Zeng L, Brody DL, Wong M. Rapamycin attenuates the development of posttraumatic epilepsy in a mouse model of traumatic brain injury. PLoS One. 2013;8:e64078.
12. Semple BD, O'Brien TJ, Gimlin K, et al. Interleukin-1 receptor in seizure susceptibility after traumatic injury to the pediatric brain. J Neurosci. 2017;37:7864–77.
13. Levin HS, Amparo E, Eisenberg HM, et al. Magnetic resonance imaging and computerized tomography in relation to the neurobehavioral sequelae of mild and moderate head injuries. J Neurosurg. 1987;66:706–13.
14. Levin HS, High WM, Goethe KE, et al. The Neurobehavioural Rating Scale: assessment of the behavioural sequelae of head injury by the clinician. J Neurol Neurosurg Psychiatry. 1987;50: 183–93.
15. Curia G, Levitt M, Fender JS, Miller JW, Ojemann J, D'Ambrosio R. Impact of injury location and severity on posttraumatic epilepsy in the rat: role of frontal neocortex. Cereb Cortex. 2010;21: 1574–92.
16. Pohlmann-Eden B, Bruckmeir J. Predictors and dynamics of posttraumatic epilepsy. Acta Neurol Scand. 1997;95:257–62.
17. Englander J, Bushnik T, Duong TT, et al. Analyzing risk factors for late posttraumatic seizures: a prospective, multicenter investigation. Acta Phys Med Rehabil. 2003;84:365–73.
18. Manley GT, Binder D, Papadopoulos M, Verkman A. New insights into water transport and edema in the central nervous system from phenotype analysis of aquaporin-4 null mice. Neuroscience. 2004;129:981–9.
19. Verkman A, Binder DK, Bloch O, Auguste K, Papadopoulos MC. Three distinct roles of aquaporin-4 in brain function revealed by knockout mice. Biochim Biophys Acta. 2006;1758:1085–93.
20. Tait MJ, Saadoun S, Bell BA, Papadopoulos MC. Water movements in the brain: role of aquaporins. Trends Neurosci. 2008;31:37–43.
21. Nagelhus EA, Ottersen OP. Physiological roles of aquaporin-4 in brain. Physiol Rev. 2013;93:1543–62.
22. Ma T, Yang B, Gillespie A, Carlson EJ, Epstein CJ, Verkman A. Generation and phenotype of a transgenic knockout mouse lacking the mercurial-insensitive water channel aquaporin-4. J Clin Invest. 1997;100:957–62.
23. Saadoun S, Tait MJ, Reza A, et al. AQP4 gene deletion in mice does not alter blood–brain barrier integrity or brain morphology. Neuroscience. 2009;161:764–72.
24. Li J, Patil RV, Verkman A. Mildly abnormal retinal function in transgenic mice without Muller cell aquaporin-4 water channels. Invest Ophthalmol Vis Sci. 2002;43:573–9.
25. Solenov E, Watanabe H, Manley GT, Verkman A. Sevenfold-reduced osmotic water permeability in primary astrocyte cultures from AQP-4-deficient mice, measured by a fluorescence quenching method. Am J Physiol Cell Physiol. 2004;286:C426–32.
26. Binder DK, Papadopoulos MC, Haggie PM, Verkman A. In vivo measurement of brain extracellular space diffusion by cortical surface photobleaching. J Neurosci. 2004;24:8049–56.
27. Binder DK, Yao X, Zador Z, Sick TJ, Verkman AS, Manley GT. Increased seizure duration and slowed potassium kinetics in mice lacking aquaporin-4 water channels. Glia. 2006;15(53):631–6.
28. Lee DJ, Hsu MS, Seldin MM, Arellano JL, Binder DK. Decreased expression of the glial water channel aquaporin-4 in the intrahippocampal kainic acid model of epileptogenesis. Exp Neurol. 2012;235:246–55.
29. Binder DK, Nagelhus EA, Ottersen OP. Aquaporin-4 and epilepsy. Glia. 2012;60:1203–14.
30. Lapato AS, Szu JI, Hasselmann JPC, Khalaj AJ, Binder DK, Tiwari-Woodruff SK. Chronic demyelination-induced seizures. Neuroscience. 2017;346:409–22.
31. Paxinos G, Franklin K. The Mouse Brain Atlas in Stereotaxic Coordinates. San Diego, CA: Academic Press; 2001.
32. Szu JI, Chaturvedi S, Patel DD, Binder DK. Aquaporin-4 dysregulation in a controlled cortical impact injury model of posttraumatic epilepsy. Neuroscience. 2020;428:140–53.
33. Reid IC, Stewart CA. Seizures, memory and synaptic plasticity. Seizure. 1997;6:351–9.
34. Ben-Ari Y. Cell death and synaptic reorganizations produced by seizures. Epilepsia. 2001;42:5–7.
35. Skucas VA, Mathews IB, Yang J, et al. Impairment of select forms of spatial memory and neurotrophin-dependent synaptic plasticity by deletion of glial aquaporin-4. J Neurosci. 2011;31:6392–7.
36. Eid T, Lee T-SW, Thomas MJ, et al. Loss of perivascular aquaporin 4 may underlie deficient water and K+ homeostasis in the human epileptogenic hippocampus. Proc Natl Acad Sci U S A. 2005;102:1193–8.
37. Lee TS, Eid T, Mane S, et al. Aquaporin-4 is increased in the sclerotic hippocampus in human temporal lobe epilepsy. Acta Neuropathol. 2004;108:493–502.
38. Alvestad S, Hammer J, Hoddevik EH, et al. Mislocalization of AQP4 precedes chronic seizures in the kainate model of temporal lobe epilepsy. Epilepsy Res. 2013;105:30–41.
39. Kim J-E, Ryu HJ, Yeo S-I, et al. Differential expressions of aquaporin subtypes in astroglia in the hippocampus of chronic epileptic rats. Neuroscience. 2009;163:781–9.

40. Kim J-E, Yeo S-I, Ryu HJ, et al. Astroglial loss and edema formation in the rat piriform cortex and hippocampus following pilocarpine-induced status epilepticus. J Comp Neurol. 2010;518:4612–28.
41. Ren Z, Iliff JJ, Yang L, et al. 'Hit & run' model of closed-skull traumatic brain injury (TBI) reveals complex patterns of post-traumatic AQP4 dysregulation. J Cereb Blood Flow Metab. 2013;33:834–45.
42. Wetherington J, Serrano G, Dingledine R. Astrocytes in the epileptic brain. Neuron. 2008;58:168–78.
43. Watrous AJ, Fried I, Ekstrom AD. Behavioral correlates of human hippocampal delta and theta oscillations during navigation. J Neurophysiol. 2011;105:1747–55.
44. Szu JI, Binder DK. The role of astrocytic aquaporin-4 in synaptic plasticity and learning and memory. Front Integr Neurosci. 2016;10:8.
45. Yao X, Uchida K, Papadopoulos MC, Zador Z, Manley GT, Verkman AS. Mildly reduced brain swelling and improved neurological outcome in aquaporin-4 knockout mice following controlled cortical impact brain injury. J Neurotrauma. 2015;32:1458–64.

How to cite this article: SzuJI, Patel DD, Chaturvedi S, Lovelace JW, Binder DK. Modulation of posttraumatic epileptogenesis in aquaporin-4 knockout mice. *Epilepsia*. 2020;00:1–12. https://doi.org/10.1111/epi.16551